Water Resources Research

RESEARCH ARTICLE
10.1029/2019WR026857

Special Section:
Coastal Hydrology and Oceanography

A Geochemical Record of Late-Holocene Hurricane Events From the Florida Everglades

Qiang Yao[1], Kam-biu Liu[1], Erika Rodrigues[2], Thomas Bianchette[3], Alejandro Antonio Aragón-Moreno[1], and Zhenqing Zhang[4]

[1]Department of Oceanography and Coastal Sciences, College of the Coast and Environment, Louisiana State University, Baton Rouge, LA, USA, [2]Laboratory of Coastal Dynamics, Graduate Program of Geology and Geochemistry, Federal University of Pará, Belém, PA, Brazil, [3]Department of Natural Sciences, College of Arts, Sciences, and Letters, University of Michigan-Dearborn, Dearborn, MI, USA, [4]School of Geographic and Environmental Sciences, Tianjin Normal University, Tianjin, China

Abstract A 5.25-m sediment core SRM-1 and 45 surface samples from mangrove forests at the Shark River Estuary in the Everglades National Park, Florida, were examined by using X-ray fluorescence and carbon isotopic analyses to study the history of intense hurricane landfall during the Late-Holocene. Significance testing of the surface samples in relation to storm deposits from Hurricane Wilma suggests that elemental concentration of Sr and Cl and the ratio of Cl/Br are the most sensitive indicators for major hurricane events in our study area. The geochemical data sets of core SRM-1 identified five active periods of intense hurricane activities during the last 3,500 years at ~3,400–3,000, ~2,200–1,500, ~1,000–800, ~600–300, and ~150 calibrated years before present to present. This is the longest paleohurricane record to date from South Florida. Our results are consistent with the view that intense hurricane activities in South Florida were modulated by Intertropical Convergence Zone (ITCZ) movements, El Niño/Southern Oscillation (ENSO) activities, and North Atlantic Oscillation (NAO) strength. This study contributes to the methodological advancement in paleotempestological studies by demonstrating that geochemical signals, particularly signals of saltwater intrusions, can be preserved in the sediment profiles on millennial time-scale and measured by X-ray fluorescence techniques, thereby enabling more storm records to be produced from otherwise suboptimal sand-limited coastal systems such as the Florida Everglades. More work needs to be done to explore the use of geochemical and stable isotopic analyses in detecting storm signals from sand-limited coastal environments.

Plain Language Summary This study uses geochemical analyses to detect intense hurricanes that made landfall near the southwest coast of the Florida Everglades from sediment profiles. The geochemical data sets identified five active periods of intense hurricane activities during the last 3,500 years at ~3,400–3,000, ~2,200–1,500, ~1,000–800, ~600–300, and ~150 years ago. Results from this study agree with previous studies that intense hurricane activities in the western Atlantic Basin were controlled by the position of ITCZ, ENSO activities, and NAO strength.

Key Points:
- This study demonstrates the use of XRF analysis in detecting major hurricane events in sand-limited coastal systems
- Five active hurricane periods were identified at ~3,400–3,000, ~2,200–1,500, ~1,000–800, ~600–300, and ~150 cal yr BP to present
- This study suggests that intense hurricane activities in the western Atlantic Basin were modulated by ITCZ, ENSO, and NAO activities

Supporting Information:
- Supporting Information S1

Correspondence to:
A. A. Aragón-Moreno and Z. Zhang,
aragonmoreno1@lsu.edu;
zhangzq@neigae.ac.cn

Citation:
Yao, Q., Liu, K., Rodrigues, E., Bianchette, T., Aragón-Moreno, A. A., & Zhang, Z. (2020). A geochemical record of Late-Holocene hurricane events from the Florida Everglades. *Water Resources Research*, *56*, e2019WR026857. https://doi.org/10.1029/2019WR026857

Received 3 DEC 2019
Accepted 24 JUL 2020
Accepted article online 27 JUL 2020

1. Introduction

Tropical cyclones, including hurricanes, are among the most devastating weather phenomena. During the last two decades, tropical cyclones have caused over 200,000 fatalities and affected the lives of over 700 million people worldwide (World Health Organization, 2020). In the Atlantic and the Eastern North Pacific Basin, hurricanes devastate the lives of tens of millions of people living in the coastal zones across the United States and Central America every year. Among the hurricane-prone regions in the United States, South Florida is particularly vulnerable to intense hurricane landfall because it can be impacted by storms coming from both the Atlantic and Gulf of Mexico (GOM) regions. According to the observational record between 1842 and 2019 CE, South Florida was struck by 36 hurricanes (National Oceanic and Atmospheric Administration [NOAA], 2019). The average return interval of hurricane landfall is ~5 years. Such unique geographical setting makes South Florida an ideal location to study the behavior of North Atlantic hurricanes. In particular, along the coastlines of the Everglades National Park (ENP), approximately 144,000 ha of protected wetlands occupy the coastal zones from Naples to Florida Bay (Lodge, 2016; Simard et al., 2006). The sediment profiles of these undisturbed

coastal wetlands started to accumulate since over 5,000 years ago (Yao & Liu, 2017; Yao et al., 2015), providing pristine archives to study the long-term pattern of hurricane landfall since the mid-Holocene, far beyond the instrumental record.

Paleotempestology, a relatively young field in the geosciences (Liu, 2004, 2013; Liu & Fearn, 1993, 2000), provides the best means to reconstruct the occurrence of paleohurricane events from the proxy record and predict the future variabilities in hurricane frequency. However, paleohurricane proxy records are remarkably rare from the densely populated South Florida coasts (Ercolani et al., 2015), and few well-dated storm records longer than 1,000 years in length exist in the region (Glaser et al., 2013; Van Soelen et al., 2012). The dearth of paleohurricane record is partially due to the sand-limited coastal wetland environment in South Florida, which has posed a challenge to the application of conventional methodology in paleotempestology.

Traditionally, the identification of storm surge deposits has been achieved by using a combination of physical indicators (e.g., % water, % organics, % carbonates, and grain size). In particular, the most useful proxy for paleotempestological studies to date has been overwash sand layers preserved in sediment cores retrieved from backbarrier lakes and marshes along the coastal zones (e.g., Brandon et al., 2013; Bregy et al., 2018; Donnelly & Woodruff, 2007; Donnelly et al., 2001; Gao et al., 2019; Lane et al., 2011; Liu, 2004, 2013; Mann et al., 2009; Wallace et al., 2014; Wallace & Anderson, 2010; Woodruff et al., 2008; Yao et al., 2018; Zhou et al., 2017, 2019). However, the usefulness of this sedimentological proxy may be problematic in a sand-limited or peat-dominated coastal environment, such as the Florida Everglades (Lodge, 2016). Previous studies have indicated that sediment profiles retrieved from the coastal Everglades consist of primarily peat deposits (>50% organic matters) with very little clastic materials (Yao & Liu, 2017; Yao et al., 2015). Accordingly, the use of geochemical proxies, such as X-ray fluorescence (XRF) and isotopic analyses, should be explored.

XRF analysis is a noninvasive geochemical analytical technique that can be used to quantify many of the common chemical elements in coastal sediments. This technique has been successfully used to detect marine-originated sediments in coastal environments and to identify some potential indicators (e.g., Ca, Sr, Cl, and Cl/Br) of storm or tsunami deposits in sediment cores (Bianchette et al., 2016; McCloskey & Liu, 2012a, 2012b, 2013; McCloskey et al., 2015, 2018; Naquin et al., 2014; Ramírez-Herrera et al., 2012; Yao et al., 2019). Given the sedimentological condition of South Florida (Yao & Liu, 2018) and site-specificity of storm sedimentation processes (Williams & Liu, 2019; Yao et al., 2019), identifying the sensitive chemical indicators for storm deposits is the key to accurately detecting paleohurricane events in sediment profiles from the region. However, the existing data sets lack robust significance testing of the XRF parameters in relation to a modern hurricane.

In addition, the use of carbon isotopic analysis in paleotempestological studies should also be explored. Because various sources of carbon show distinct differences in carbon isotopic ratios ($\delta^{13}C$) and organic carbon to total nitrogen ratios (C/N), variations in $\delta^{13}C$ and C/N have been used to describe the origin of organic materials preserved in coastal environments (Chmura & Aharon, 1995; Lamb et al., 2006; Lambert et al., 2008). In a peat-dominated coastal environment such as the Everglades, these isotopic indicators are expected to be more sensitive in detecting the marine incursion events in regard to the conventional sedimentological proxy used in previous paleotempestological studies. However, among long-term hurricane records from Florida, few attempts have been made in using carbon isotopic analysis to detect paleohurricane events in sediment profiles (Das et al., 2013; Lambert et al., 2008).

In this paper, we aim to fill the above-mentioned data gaps and explore the use of XRF and isotope analyses to identify paleohurricane events in Southwest Florida based on 45 surface samples and a 5.25-m sediment core (SRM-1) retrieved in the ENP. The surface samples were taken along a 20-km transect with distinct marine-to-terrestrial gradient and core SRM-1 contains over 5,700 years of sedimentary history including ~10 cm of distinctive storm deposit attributable to Hurricane Wilma (2005) at the top of the core. The main objectives of this study are to (1) reveal the hurricane indicators in a peat-dominated coastal environment by characterize the chemical signature of Hurricane Wilma deposits, (2) identify evidence of intense paleohurricane events during the Late-Holocene in the sedimentary record, and (3) reconstruct the history of paleohurricane strikes in the Shark River Slough in the context of Late-Holocene environmental changes in the Florida Coastal Everglades.

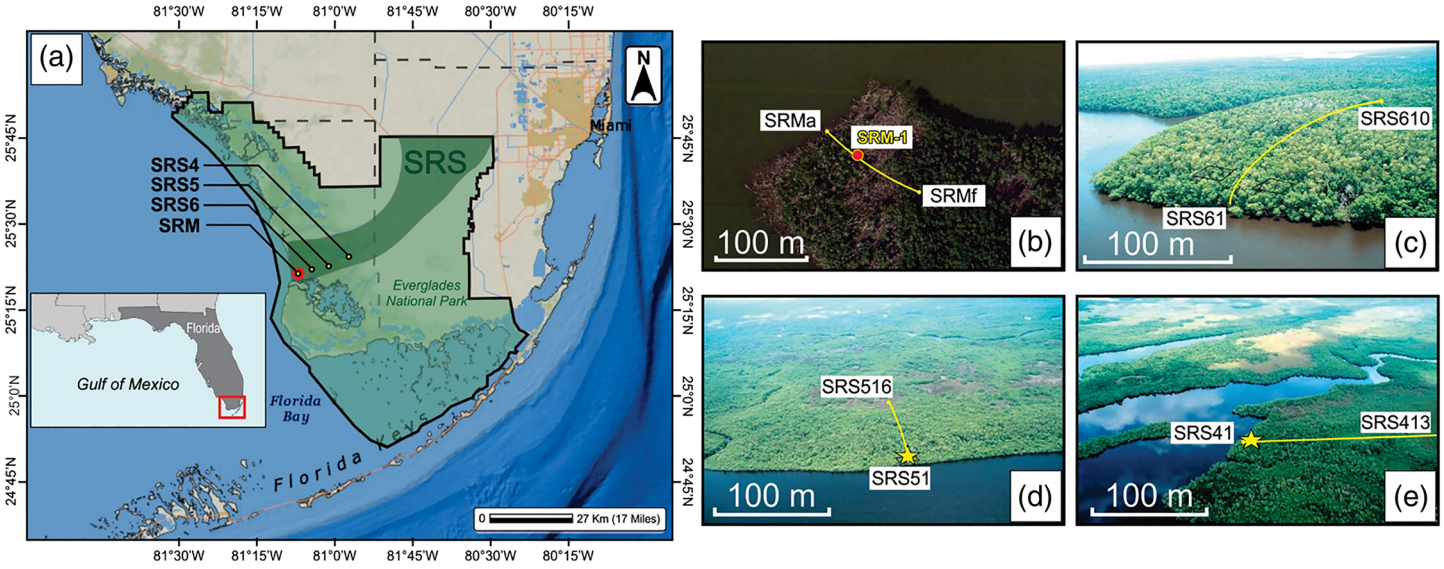

Figure 1. (a) Location of core SRM-1 and surface sample transects in the Everglades National Park, South Florida. (b) The yellow line indicates the transect where surface samples SRMa to SRMf were taken. The red dot points to core SRM-1. (c) Transect SRS6 where surface samples SRS61 to SRS610 where taken. (d) transect SRS5 where surface samples SRS51 to SRS516 were taken. (e) Transect SRS4 where surface samples SRS41 to SRS413 were taken. See Table S1 for more details about the surface samples.

2. Materials and Methods

2.1. Study Area

The coring site for SRM-1 (25°21′10″N, 81°6′52″W) is located on the edge of Ponce de Leon Bay, at the coastal junction where the Shark River Slough, the largest slow-moving flow of freshwater in the Florida Everglades, meets the saltwater of the GOM (Figure 1). Historically, water overflowing Lake Okeechobee and associated rainfall result in a southward sheet flow along a gentle slope of ~3 cm/km down Shark River Slough into the GOM (Lodge, 2016). The 45 surface samples were taken from 4 main study areas (SRM, SRS-6, SRS-5, and SRS-4) along the Shark River Slough (Figure 1). Site SRM is situated at the mouth of the Shark River Slough, and sites SRS-6, SRS-5, and SRS-4 are part of the Florida Coastal Everglades Long-term Ecological Research (LTER) sites situated at approximately 4 km, 8 km, and 20 km upstream from SRM, respectively. The four study areas are located along a distinct marine-to-terrestrial transect. Accordingly, the overall salinity, though fluctuating overtime due to tidal and seasonal changes, decreases significantly upstream from SRM (>30 ppt) to SRS-6 (27 ± 2.6 ppt), SRS-5 (20.8 ± 3.1 ppt), and SRS-4 (4.6 ± 1.1 ppt). The Global Positioning System (GPS) and salinity data of all the surface samples can be found in Table S1 in the supporting information.

Recent studies from the Shark River Slough indicate that our study areas were situated on a dry and upland environment before the mid-Holocene (Yao & Liu, 2017). As a result of the rapid sea level rise and increasing water table in South Florida, freshwater marsh started to appear at the Shark River Mouth (SRM) during the mid-Holocene (Yao et al., 2015). As marine transgression continued between 5,700 and 3,500 calibrated years before present (cal yr BP), brackish marsh started to appear at the SRM area and freshwater marsh progressively expanded inland and upstream from site SRM to SRS-4 along the Shark River Slough (Yao & Liu, 2017, 2018). At ~3,500 cal yr BP, due to the establishment of mangrove forests and decelerating sea level rise (<0.4 mm/year after ~3,500 cal yr BP), marine transgression has stabilized at coastlines along South Florida (Parkinson, 1989; Scholl et al., 1969; Wanless et al., 1994). During the next 2,000 years, mangroves continue to expand and a dense *Rhizophora mangle*-dominated mangrove forest was formed at the mouth of the Shark River Slough at ~1,150 cal yr BP, when the shoreline reached its modern position at the Shark River Estuary (Yao et al., 2015). Pollen and sedimentary record shows that since ~1,150 cal yr BP, site SRM has been sitting on a fringing mangrove forest, where *Laguncularia racemosa* (white mangrove) and *Rhizophora mangle* (red mangrove) are co-dominant species and *Avicennia germinans* (black mangrove) is also present. The hydroperiod in the study site is influenced mainly by tidal cycles. Accordingly, the

mangrove forests at the study area are inundated by tides 90% of the year, with an average tidal range of 0.5 m (Yao et al., 2015), and soil pore-water salinity is ~30 ppt (Yao & Liu, 2017).

Studies have shown that hurricanes play an important role in regulating the structure of mangrove forests at the mouth of Shark River Slough (Chen & Twilley, 1999a, 1999b; Smoak et al., 2013). Mineral and sediment inputs during storm events from the GOM, rather than inputs from upland, enhance nutrient concentrations in the coastal area, causing higher biomass and tree height in the fringing mangrove forest (SRM and SRS-6) in contrast to upstream sites (SRS 5 and SRS-4) of this estuary and other regions of southeastern Florida (Castañeda-Moya et al., 2010, 2013, 2020). Hence, the average height of mangroves trees at site SRM are among the highest in southwestern Florida (>25 m) (Simard et al., 2006).

2.2. Historical Hurricanes and Their Meteorological Characteristics

Instrumental record shows that three hurricanes struck near our study area (within 100 km of core SRM-1) during the nineteenth century (NOAA, 2019). From 1901 to 2019 CE, 15 intense hurricanes (categories 3–5 according to the Saffir-Simpson scale) have made landfall near our study area (within 100 km), an average return interval of ~8 years (NOAA, 2019) (Figure 2). During the twentieth century, prior to the retrieval of core SRM-1 (May 2010), two category 5 storms, the Labor Day Hurricane and Hurricane Andrew, directly struck South Florida in 1935 and 1992 (Elsner & Kara, 1999). The Labor Day Hurricane was the first recorded category 5 hurricane to hit the United States. It crossed the middle Florida Keys, then moved northward parallel to the west Florida coastlines and made landfall near Cedar Key, approximately 460 km north of our study site (Smith et al., 2009). There are no estimates of storm surge and damage at our study area from this storm. Andrew made landfall on the southeast coast of the Florida peninsula as a category 5 hurricane and exited into the GOM at ~30 km north to our study site as a category 4 hurricane (Landsea et al., 2004). Although Andrew's track was very close to our study area, it had a compact eye of ~15 km in radius (Mayfield et al., 1994). The storm surge deposited sediment along a 13-km length of coast from Highland Beach to Shark Point (Risi et al., 1995), just a few kilometers north of our study site.

Hurricane Wilma was the most recent intense hurricane that made landfall near our study area prior to the retrieval of core SRM-1 (May 2010). Compared with Andrew, the track of Wilma was farther away from our study site (Figure 2). It approached South Florida from the southwest and made landfall as a category 3 hurricane on 24 October 2005 near Everglades City, ~60 km north of our study site (Smith et al., 2009). However, Wilma had an extremely large eye (a radius of ~50 km) at landfall, with the northern eyewall passing south of Naples and the southern eyewall passing approximately 10 km south of our study site (Zhang et al., 2008). It deposited up to 10 cm of sediment as far as 10 km inland from the GOM along a 70-km stretch of coastline from Lostmans River to Flamingo (Castañeda-Moya et al., 2010; Smith et al., 2009). When the storm passed our study area, the wind speed was 46 m/s and the storm surge was 3–4 m (Castañeda-Moya et al., 2010). Hence, Wilma deposited approximately 10 cm of marine sediments on top of the mangrove forest at site SRM and SRS-6 (Figure 3) (Castañeda-Moya et al., 2010; Smoak et al., 2013). As the storm surge weakened toward the upstream areas of the Shark River Slough, storm deposits of Hurricane Wilma gradually faded at site SRS-5 and were absent at site SRS-4 (Castañeda-Moya et al., 2010; Yao & Liu, 2017). Strong winds and storm surge from Wilma caused significant damages including defoliation, tree snapping, and uprooting to approximately 1,250 ha of mangrove forest along the west coast of the ENP, resulting in 90% mortality of trees with diameters at breast height greater than 2.5 cm (Smith et al., 2009; Whelan et al., 2009).

The sensitivity of a study site to register evidence of hurricane strikes is affected by several geomorphological and meteorological factors such as storm intensity, storm surge height, site-to-sea distance, and direction of the landfalling storm (Liu, 2004, 2007; Liu & Fearn, 1993, 2000). It is important to note that in the northern hemisphere, the peak storm surge occurs along the forward-right quadrant of the landfalling hurricane (Liu, 2004, 2007). Therefore, storm surge heights are greater on the right side of the landfalling hurricane because of the stronger onshore winds, and more subdue on the left side due to prevalence of the offshore winds (Simpson & Riehl, 1981). Previous paleohurricane studies have suggested that the proxy record is more sensitive to major hurricanes (category 3 intensity and above) making landfall immediately to the west of the study site (i.e., landfall within 50-km radius) (Liu, 2004, 2013; Liu & Fearn, 1993, 2000). Therefore, hurricanes and winter storms that made landfall at the Atlantic Coast or Florida Keys likely will not cause marine incursions detectable in proxy records from the Shark River Estuary. Although 15 hurricanes struck the Everglades since the twentieth century, only four made landfalls immediately to the north of our study

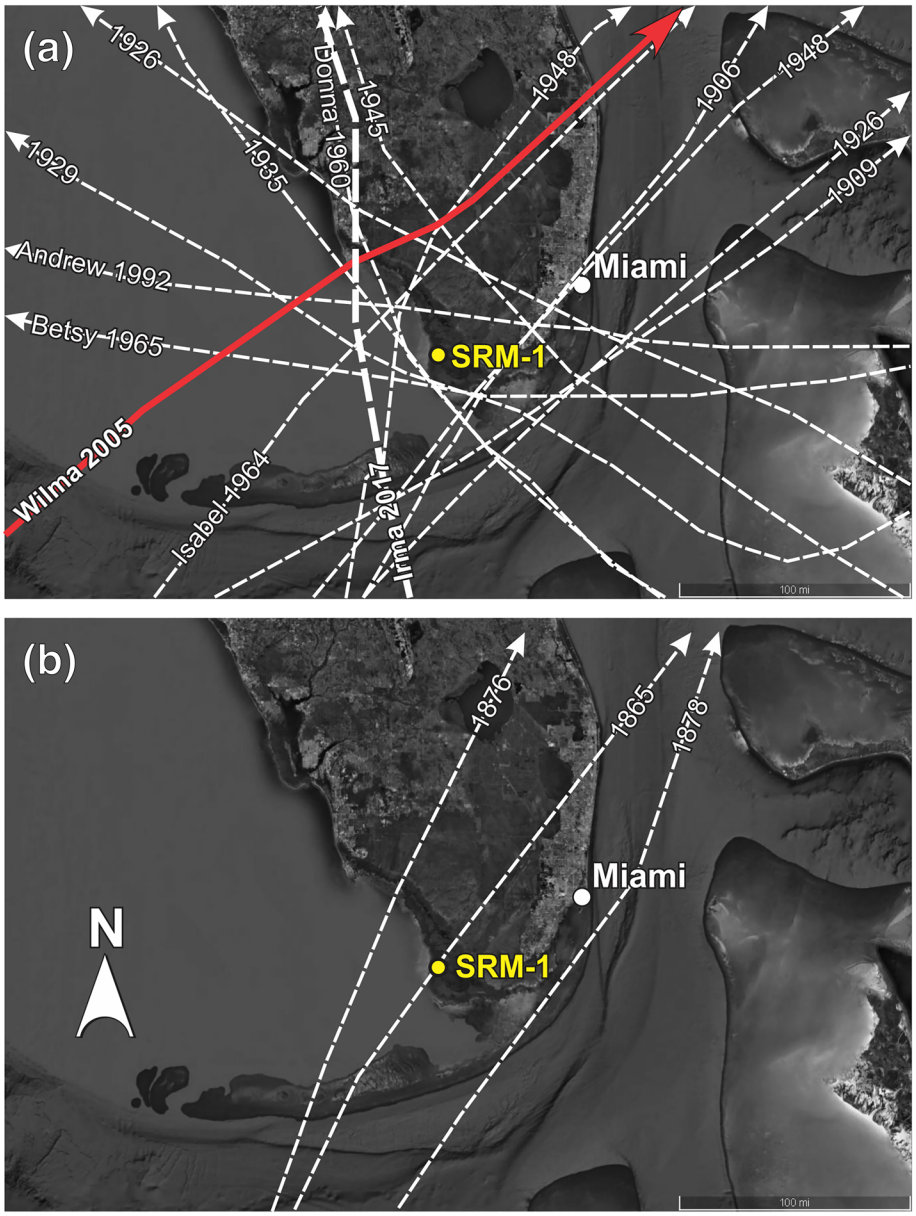

Figure 2. Aerial image of hurricane landfalls in South Florida near our study site (within 100 km). (a) Fifteen intense hurricanes (category 3–5 according to the Saffir-Simpson scale) from CE 1900 to 2019. (b) All recorded hurricanes before CE 1900. The arrows indicate the direction of the hurricane (figures modified from National Oceanic and Atmospheric Administration, Historical Hurricane Tracks website: https://coast.noaa.gov/hurricanes/).

site prior to the coring date (Hurricane Donna, Isbell, Wilma, and the 1948 hurricane) (Figure 2). Among these four hurricanes, Donna (1960) was a category 3 hurricane at landfall (Houston & Powell, 2003). It traveled parallel to the coastlines of our study area, and struck near Naples and Fort Myers, Florida (Dunn & Miller, 1961). As a result, higher storm surge and damages occurred at the Everglades City (~75 km north of our study site) but not at the Shark River Slough (Craighead & Gilbert, 1962; Smith et al., 2009). Isbell (1964) made landfall as a Category 2 hurricane at ~60 km north of our study site (Dunn, 1965), and no major storm surge was reported (Dunn, 1965). The 1948 hurricane was very similar to hurricane Isbell in its path and intensity (NOAA, 2019). Therefore, it is likely that Hurricane Wilma, being a stronger and more recent storm with a more direct impact at our study site, is the only storm that is individually distinguishable in the sediment profiles from the Shark River Estuary among the 15 major hurricanes recorded in the instrumental record.

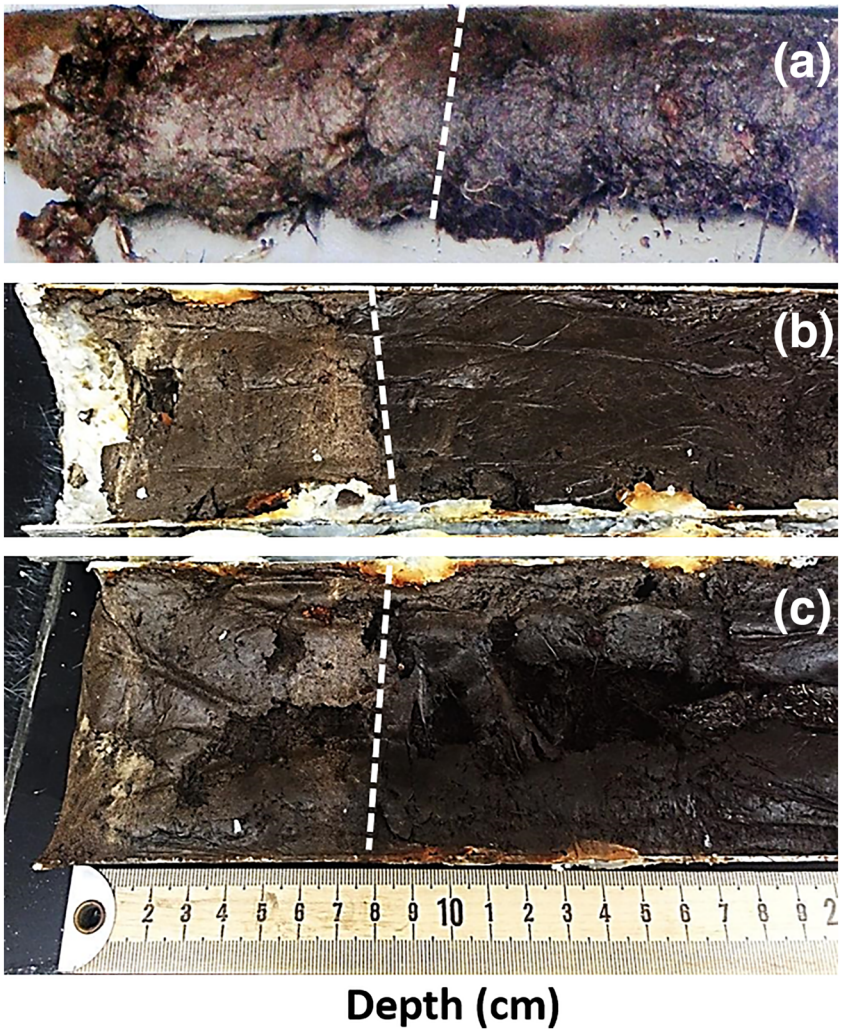

Figure 3. Uppermost sedimentary unit of (a) core SRM-1, (b) aluminum push core 1, and (c) aluminum push core 2. Eight to ten centimeters of storm deposits (above the white dash line) from Hurricane Wilma are found at the top of all cores overlying the peat sediments.

Given the depositional and sea level history of our study area, it is reasonable to believe that the relative site-to-sea distance at site SRM has been sensitive enough to register major hurricane events since ~3,500 cal yr BP, when shoreline retreat stabilized at the Shark River Estuary (Yao & Liu, 2017, 2018). Although the sediment profile at the study area recorded over ~5,700 years of paleoecological history (Yao et al., 2015), a combination of XRF and isotope analyses is expected to provide a conservative, minimal record of intense hurricanes events over the last 3,500 years from core SRM-1. The significance testing of the 45 surface samples from a transect with progressively thinning Hurricane Wilma deposits (Figure 1) will reveal the sensitivity of various geochemical parameters in relation to marine incursion events.

2.3. Methods

2.3.1. Core and Surface Sample Extraction

In this study, a 525-cm core (SRM-1) was retrieved using a Russian peat borer along with two 50-cm aluminum push cores at mouth of the Shark River Slough (site SRM) in May 2010 (Figure 1). In addition, 45 surface samples were also collected following the channel of the Shark River Slough along a distinct marine-to-terrestrial gradient (Table S1 and Figure 1) (Castañeda-Moya et al., 2010; Yao & Liu, 2018). The surface samples were taken from four main study sites (SRM, SRS-6, SRS-5, and SRS-4) ranging from the mouth of the Shark River Slough to ~20 km upstream. At each site, 6 to 16 surface samples were taken

along a secondary gradient perpendicular to the river as a function of the distance away from the river (Figure 1), which acts as a conduit of storm surge and storm deposits from the sea (Castañeda-Moya et al., 2010; Chen & Twilley, 1999a, 1999b; Yao & Liu, 2018). A total of 18 samples was collected from the four main study sites. Salinity data for site SRS-6 to SRS-4 were retrieved from our collaborators (Castañeda-Moya et al., 2010, 2013, 2020). Salinity data for site SRM were measured during our field expedition in May 2010. The surface samples were collected by first removing plant litter and debris from the surface ground, and then collecting up to 5 cm of upper soil by using a small hand shovel.

2.3.2. Laboratory Analyses

In the laboratory, XRF analysis was performed on all surface samples as well as on core SRM-1 at 2-cm intervals by using an Olympus Innov-X DELTA Premium XRF analyzer, which measures the elemental concentrations of 25+ elements (units are reported in part per million) with an atomic number larger than 15. A total of 15 elements were detected in our samples, but 7 of them were in traceable amount with no systematic changes. Therefore, eight common chemical elements (Ca, Sr, S, Fe, Cl, Ti, Zr, and Br) and Cl/Br ratio were reported in this study (Figure 5).

In addition, 95 samples throughout core SRM-1 at 2- to 5-cm intervals were sent to Stable Isotope Facility at the University of California, Davis for Total Organic Carbon (TOC), $\delta^{13}C$, and C/N measurements. All the samples consist of bulk sediments. Pretreatment was performed in LSU Global Paleoecology Laboratory, where samples were bathed in 2 ml of 10% HCL, treated in ultrasonic tank for 5 min, and washed with distilled water and centrifuged for three times for 4 min each. In UC Davis Stable Isotope Facility, samples were analyzed using a PDZ Europa ANCA-GSL elemental analyzer interfaced to a PDZ Europa 20-20 isotope ratio mass spectrometer (Sercon Ltd., Cheshire, UK). The isotope data are expressed on a Vienna Pee Dee Belemnite (VPDB) scale.

Standardization of the selected data set was used to filtered the "background noises" from sea-level fluctuations and small-scale events and amplify the chemical signals of intense hurricanes. Normalized values of $\delta^{13}C$, C/N, and selected XRF data were calculated using Z values (Salkind, 2010). First, we subtracted the mean value of each data set to each score, and then we divided each result by the standard deviation of the data set. The standardized data set was presented to identify periods with higher variability and be comparable with other studies with different proxies. In this paper we focus on the top 445 cm of the core because it contains the depositional history of the peat-forming coastal wetlands that is relevant to the reconstruction of paleohurricane activities.

2.3.3. Statistical Analyses

Principal component analysis (PCA) was performed by using the C-2 version 1.8 (species transformation: log10, rotate axes, center data by variables, and standardize data by variables) on all surface samples to reveal the sensitivity of various geochemical parameters in relation to storm deposits from a modern hurricane event. The PCA results provide a basis to identify the most sensitive geochemical parameter to marine incursion events.

2.3.4. Chronology

Fourteen samples from core SRM-1 were sent to NOSAMS Laboratory at Woods Hole Oceanographic Institution and Beta Analytic Inc., in Miami, Florida, for AMS ^{14}C measurements. The chronology of core SRM-1 was developed by using BACON version 2.2 (Blaauw & Christen, 2013) and has been previously established (Yao et al., 2015). The accumulation rate priors are based on default settings (acc.shape = 1.5, res = 5, mem.strength = 4, and mem.mean = 0.7), except for prior distributions (acc.mean = 10). The ages described in this paper are reported as cal yr BP. Because the top 10 cm of the clastic sediments at our study site has been attributed to sediments deposited by Hurricane Wilma in 2005 and published in many studies (Castañeda-Moya et al., 2010; Smith et al., 2009; Smoak et al., 2013; Yao & Liu, 2017; Yao et al., 2015), we used 10–11 cm from the top of core SRM-1 as −55 cal yr BP (1950 CE as 0 cal yr BP) to run the model in BACON version 2.2 (Figure 4). More information of ^{14}C samples are described in Table S2.

3. Results

3.1. Chronology

Among the 14 AMS ^{14}C dates obtained from NOSAMS and Beta Analytic, three anomalously young dates retrieved at 246 and 440 cm are rejected due to extreme stratigraphic reversal (Table S2). The surface (0 cm

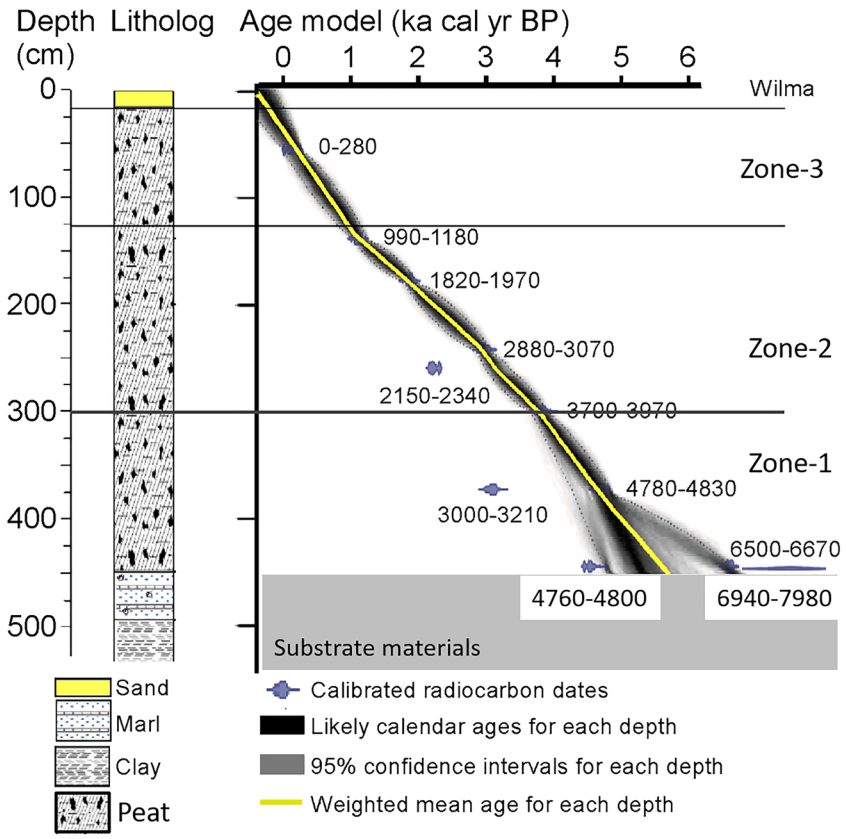

Figure 4. Lithology and the age-depth model for core SRM-1. The age-depth model is developed by BACON and based on 11 calibrated C^{14} ages (2-σ calibrated range). The yellow curve shows the 'highest probability' estimated age for each depth based on the weighted mean age.

at −55 cal yr BP) and 11 valid ^{14}C dates were used to construct the age-depth model by BACON v2.2 (Figure 4). The result shows that the highest probability age-depth model (yellow curve) based on weighted mean age of each depth is very close to a polynomial line intercepting ^{14}C dates at 56 (178 cal yr BP), 139 (1,138 cal yr BP), 179 (1872 cal yr BP), 243 (2,947 cal yr BP), 300 (3,777 cal yr BP), and

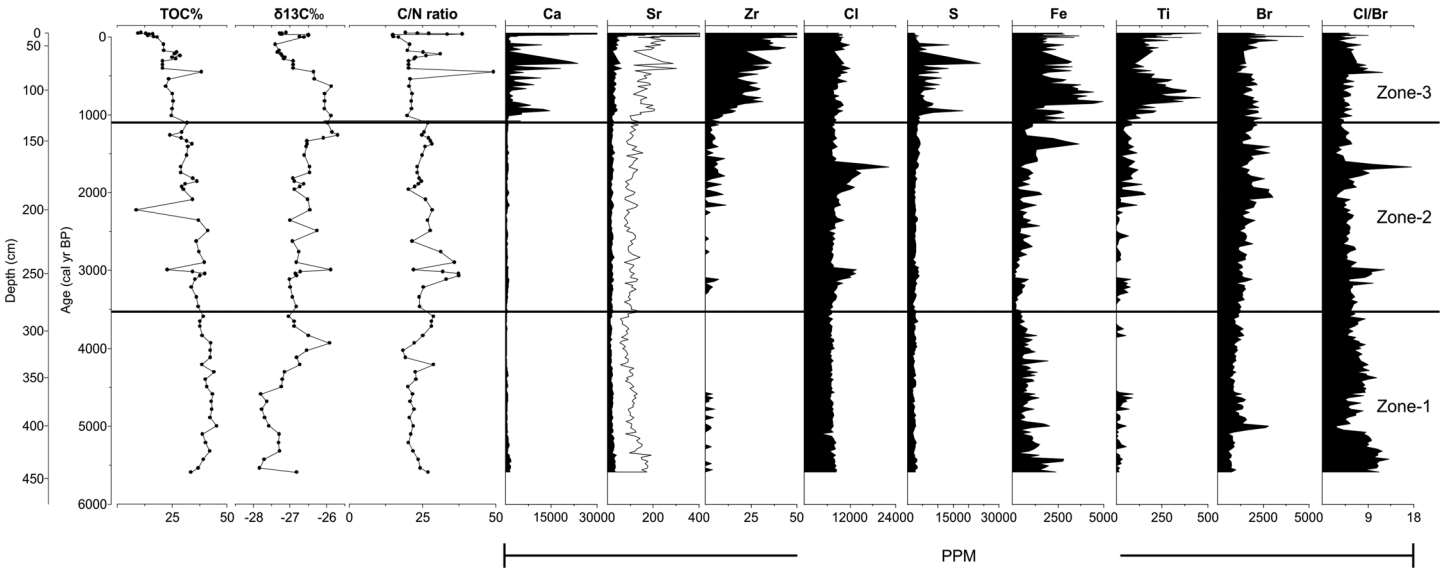

Figure 5. The TOC%, $\delta^{13}C$, C/N, and XRF diagram of core SRM-1.

374 (4,658 cal yr BP) cm. We picked a basal date of 5,674 cal yr BP at 450 cm based on estimation of the highest probability age-depth model. More detailed description of the chronology of core SRM-1 can be seen in Yao et al. (2015).

3.2. Geochemical Proxy Results

Core SRM-1 consists of four different sediment types (Figure 4). The basal part of the core consists of homogeneous clay (525–485 cm) and marl (485–445 cm) deposited prior to the development of coastal marsh (Yao & Liu, 2017). Above the basal sediments are 445 cm of peat, including a 10-cm layer of calcareous clastic sediments at the top of the core (10–0 cm) (Figure 4). For this paper, we divided the core into three stratigraphic zones, based on the paleoenvironmental history of the study area (Yao & Liu, 2017; Yao et al., 2015) and chemical characteristics of core SRM-1 (Figure 5).

3.3. Zone-1 (445–300 cm, ~5,700–3,500 cal yr BP)

Pollen records from previous studies show that the vegetation at our study area was dominated by upland and marsh plants (e.g., *Pinus*, *Quercus*, *Salix*, Poaceae, and Amaranthaceae), suggesting a relatively inland and freshwater environment during this period at our coring site (SRM-1), but the shoreline was closing in due to rapid sea level rise (Yao & Liu, 2017; Yao et al., 2015). The peat sediments in this section display relatively stable geochemical signals throughout Zone-1. The XRF data show that the elemental concentrations of Ca (<1,000 ppm), S (<5,000 ppm), Cl (<10,000 ppm), and Fe (<2000 ppm) are relatively stable in most intervals throughout Zone-1. Only trace amount of Ti (<100 ppm), Sr (<50 ppm), Zr (<10 ppm), and Br (<25 ppm) are detected in some intervals in Zone-1 (Figure 5). The elemental concentrations of Ca, S, Zr, and Cl are in general the lowest throughout the core, and the Cl/Br ratio is relatively higher toward the bottom of Zone-1. In addition, Zone-1 contains the highest TOC% throughout the core. The $\delta^{13}C$ ranges from −28 to −25.5‰ and becomes more positive toward the top of the zone. The C/N ranges from 18 to 29.

3.3.1. Zone-2 (300–125 cm, ~3,500–1,150 cal yr BP)

Although marine transgression has stabilized since ~3,500 cal yr BP in South Florida (Parkinson, 1989; Scholl et al., 1969; Wanless et al., 1994), saltwater intrusion continued at our study area during the next 2,350 years as the freshwater environment gradually transit to a brackish environment and mangroves started to expand toward more inland and upstream areas of the Shark River Slough (Yao & Liu, 2017; Yao et al., 2015). The XRF data show that although still relatively low, the concentration of most elements has increased in regards to Zone-1; in particular, the concentration of Zr, Ti, and Br shows substantial increase, and abrupt increases in Cl (>15,000 ppm) and Cl/Br ratio occur at two intervals at approximately 245–260 cm (3,000–3,400 cal yr BP) and 160–180 cm (1,500–2,200 cal yr BP) (Figure 5). In addition, the TOC% gradually decreases toward the top of the zone. The $\delta^{13}C$ ranges from −27 to −25‰, and C/N ranges from 20 to 35.

3.3.2. Zone-3 (125–0 cm, 1,150 cal yr BP to Present)

The paleoenvironmental history of this period is characterized by the formation of the modern shoreline, a coastline dominated by *Rhizophora mangle*. XRF analyses show that the concentrations of all the elements are much higher than those in Zone-1 and Zone-2. In particular, the top 10 cm of the core contains exponentially higher concentrations of most elements than in the underlying peat (Figure 5). The Cl/Br ratio exhibits some fluctuations throughout Zone-3 (Figure 5). In addition, the TOC% further decreases toward the top and reaches the lowest values at the top 10 cm of the core. The values of $\delta^{13}C$ and C/N are within the similar range in regard to Zone-2 but exhibit more variations.

3.4. Numerical Analysis of Surface Samples

XRF analysis of the 45 surface samples show that samples taken from site SRM-1 and SRS-5 have higher concentration of all measured elements in regard to samples from site SRS-5 and SRS-4. In particular, samples from site SRM-1 have significantly higher Cl, S, Ti, Fe, Br, and Cl/Br ratio than all the other surface samples. Overall, the chemical richness decreases progressively from site SRM-1 to SRS-4 (Figure 6).

The XRF data of all 45 surface samples were used in PCA analysis. On the PCA biplot of the nine chemical parameters (Figure 4), the first two principal components (PC) account for 71.3% and 9.7% of the variance (Table S3). All samples from Site SRM-1 and most samples from site SRS-6 have positive scores on both PC1 and PC2 axes and are located in the upper-right quadrant of the biplot (Figure 6). Among all the

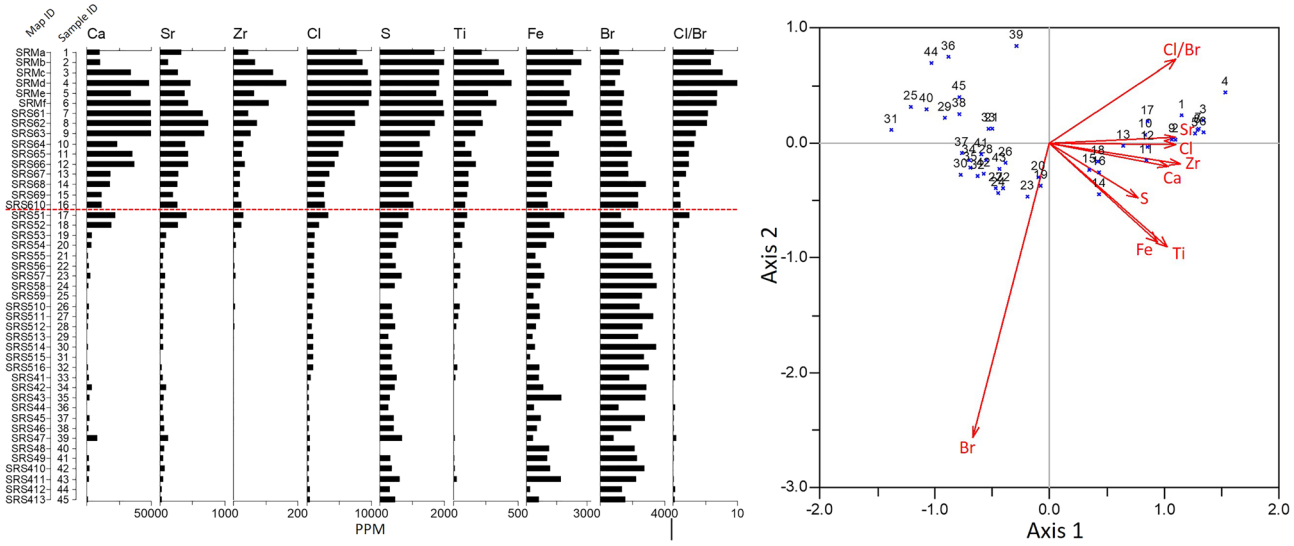

Figure 6. Left: X-ray fluorescence results of eight chemical elements and Cl/Br ratio for 45 surface samples. Samples coded to aid the identification. Same coding applies to the map and all the other figures. The red line separates samples from coastal (SRM, SRS-6) and terrestrial (SRS-5, SRS-4) sites. Right: Principal component analysis biplot showing coordinates of eight chemical elements and Cl/Br ratio from the X-ray fluorescence diagram of surface samples plotted along components 1 and 2.

variables, Cl/Br, Sr, and Cl have positive scores on both PC1 and PC2 axes and Br has negative scores on both PC1 and PC2 axes.

4. Discussion

4.1. Significance Testing of the Marine Indicators in Relation to Hurricane Wilma

Previous studies have thoroughly described that storm surge and associated deposition from Hurricane Wilma caused significant impacts to coastal areas along the Shark River Slough (site SRM and SRS-5) (Castañeda-Moya et al., 2010, 2020; Smith et al., 2009; Smoak et al., 2013; Yao & Liu, 2017, 2018; Yao et al., 2015). More importantly, Hurricane Wilma was the only major hurricane that landed directly across our study area prior to the coring date. Thus, it can be inferred that the top 10 cm of calcareous clastic sediments in core SRM-1 and surface samples from site SRM and SRS-6 are the storm deposits from Hurricane Wilma (Figures 5 and 6).

Figure 6 summarizes the geochemical characteristics of the storm deposits. Overall, the Wilma deposits have significantly higher contents of Zr, Ca, Sr, Ti, Cl, S, and Cl/Br ratio and slightly higher concentration of Fe than the underlying peat (Figures 5 and 6). In particular, significance testing of the surface samples taken along a marine-to-terrestrial gradient with gradually thinning storm signals shows that the elemental concentration of Cl and Sr and Cl/Br ratio has the closest association with storm deposits from Hurricane Wilma among the 9 XRF parameters. High content of Sr has been described as an indicator of marine incursions in previous studies from southwestern Florida (Van Soelen et al., 2012; Yao & Liu, 2018) and elsewhere (Bianchette et al., 2016; Liu et al., 2015; McCloskey et al., 2015, 2018; McCloskey & Liu, 2013; Ramírez-Herrera et al., 2012; Woodruff et al., 2009). This element is likely associated with marine gastropods in offshore environment and introduced to coastal area by storm surges (Yao & Liu, 2017; Yao et al., 2015, 2019). The ratio of Cl/Br has the highest score on both PC1 and PC2 axes; hence, it has the closest association with Wilma deposits. Many studies have revealed that although aqueous bromine (HOBr/OBr-) is one of the most abundant element in seawater, it tends to react with organic matters in terrestrial environments, due to its higher electron density and smaller bond strength (Ryu et al., 2018; Westerhoff et al., 2004). On the contrary, chlorine (HOCl/OCl-) is more abundant in inorganic environments (Donahoe et al., 1994; Tuthill et al., 1998). Hence, an increase in Cl and decrease in Br concentration has been used as evidence for marine incursion event (e.g., storm surge) in highly organic environment (e.g., coastal wetland). Furthermore, the Cl/Br ratio in seawater (655:1) (Alcalá & Custodio, 2008) is much higher than that in precipitation (100:1 to 300:1)

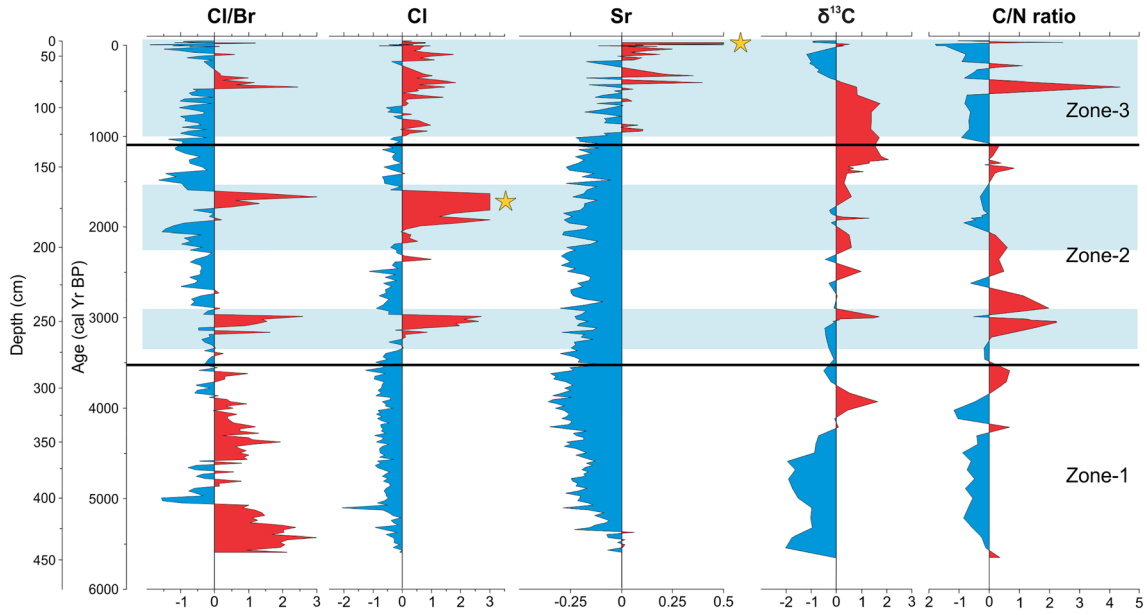

Figure 7. Cl/Br, Cl, Sr, $\delta^{13}C$, and C/N records for core SRM-1. The data have been standardized and plotted by positive (red) and negative (blue) excursions from the mean concentrations of each variable. Intervals marked by blue shades represent periods of elevated major hurricane activities (categories 3–5). The star points to intervals with exponentially high values where the curve was cut off to save space. Sediments deposited by Hurricane Wilma is represented by a thin peak of high values of Cl/Br, Sr, and C/N at the top of the core.

(Davis et al., 1998). Therefore, the Cl/Br ratio is a sensitive indicator to detect evidence of storm surge in sediment profile (Liu et al., 2015; Yao et al., 2015). In this case, unlike other common marine indicators (e.g., Zr, Ca, Sr, and S) described in previous studies (Bianchette et al., 2016; McCloskey & Liu, 2013; McCloskey et al., 2015; Ramírez-Herrera et al., 2012), the ratio of Cl/Br and the concentration of Cl is associated with saltwater intrusion caused by storm surges (Liu et al., 2015; McCloskey et al., 2018; Yao et al., 2019). More importantly, a study of Hurricane Harvey deposits from the Texas coast has demonstrated that the ratio of Cl/Br can be used to identify storm surge events in the sedimentary record in the absence of overwash processes (Yao et al., 2019). Hence, this parameter is a particularly sensitive storm indicator in sand-limited coastal systems where traditional sedimentological proxies (i.e., overwash sand layers) are absent or ineffective. Therefore, based on the significance testing of surface samples and information from previous studies, we believe that the elemental concentration of Sr and Cl and the ratio of Cl/Br are the most sensitive indicators for major hurricane events at our study area among all nine XRF parameters.

4.2. Geochemical Record of Late-Holocene Hurricane Events

Figure 7 summarizes the standardized Cl/Br, Cl, Sr, $\delta^{13}C$, and C/N data from core SRM-1. Positive excursions in Cl/Br, Sr, and Cl record are marked in red color and interpreted as potential evidence for paleohurricane activities. From ~5,700 to 3,500 cal yr BP (Zone-1), although Cl/Br record shows many intervals with positive excursions, Cl and Sr record exhibit opposite results. This inconsistency among storm indicators in the data set is likely caused by sediment compaction and different geomorphological condition during the time period (Yao & Liu, 2017; Yao et al., 2015). As discussed in previous sections, site SRM was situated in a relatively inland and freshwater environment prior to 3,500 cal yr BP. Although marine transgression was rapidly approaching in, the relative sea level in southwestern Florida was still much lower than the present level and the shoreline was ~30 km seaward relative to that of today (Parkinson, 1989; Wanless et al., 1994; Yao et al., 2015). With such site-to-sea distance, sediment profiles in Zone-1 were not sensitive enough to register any evidence of paleohurricane activities between ~5,700 and 3,500 cal yr BP. More importantly, because bromine originates almost exclusively from seawater (McCloskey et al., 2018; Westerhoff et al., 2004), it is reasonable to believe that the concentration of this element is remarkably lower in the sediment profile prior to 3,500 cal yr BP when the sea level was lower than today. Hence, the high

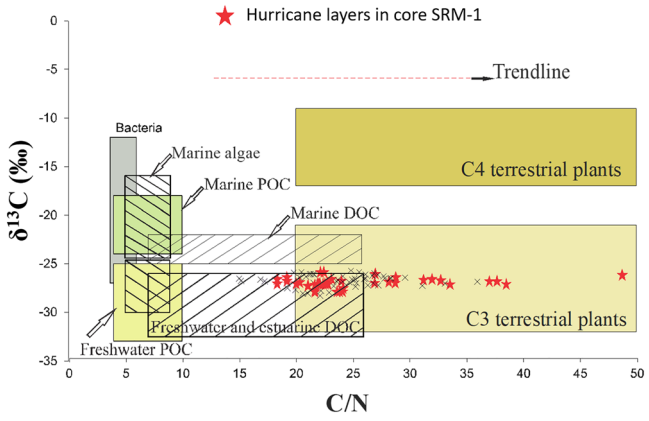

Figure 8. Typical $\delta^{13}C$ and C/N ranges for organic materials from various sources in coastal environments (Lamb et al., 2006). The red stars mark the isotope data sets of inferred storm intervals in core SRM-1. The rest of the sediment intervals in core SRM-1 are marked by "X."

Cl/Br ratio, which pervades virtually throughout the entire Zone-1, rather than episodically as in the two zones above it, is caused by the lowered Br concentrations here relative to the consistent Cl values (Figure 5). This suggests that the high Cl/Br ratio reflects the geochemical and environmental background at the site and cannot be taken as a paleohurricane proxy during these two millennia.

From 3,500 to 1,150 cal yr BP (Zone-2), although the Sr record still shows negative excursions, many intervals in the Cl/Br and Cl records show signs of marine incursions. In particular, two prominent peaks occur between 245–260 cm (~3,000–3,400 cal yr BP) and 160–180 cm (~1,500–2,200 cal yr BP) (Figure 7). We interpret that these two intervals represent two periods of elevated major hurricane activities (category 3–5). Previous observational and modeling studies suggest that major hurricanes can introduce marine water and sediments up to 10 km inland in the coastal Everglades (Castañeda-Moya et al., 2010, 2013; Chen & Twilley, 1999b; Smith et al., 2009; Smoak et al., 2013). During Zone-2, although much closer to the sea in comparison to Zone-1, our study site, which is currently at the mouth of the Shark River Slough, would still have been at some distance inland from the former shoreline and beyond the distance reachable by marine sediments carried by storm surge waters during the period from ~3,500 to 1,150 cal yr BP. This explains the negative background values of Sr, a common indicator of marine sediments (Bianchette et al., 2016; McCloskey & Liu, 2013; McCloskey et al., 2015; Ramírez-Herrera et al., 2012; Yao & Liu, 2018), throughout Zone-2. However, Cl and Cl/Br are associated more with saltwater intrusion than the delivery of marine sediments (Liu et al., 2015; McCloskey et al., 2018; Yao et al., 2019). Hence, extremely high-energy events, such as strong storm surges caused by catastrophic hurricanes (category 4 or 5), could have introduced large quantities of seawater to the coring site, and the impoundment of the storm surge water inland by natural topographic barriers is reflected by positive excursions of Cl and Cl/Br in Zone-2.

From 1,150 cal yr BP to present (Zone-3), as sea level rise has rendered the study site a truly coastal location subjected to storm surge deposition (Yao et al., 2015), intervals with positive excursion of Cl/Br, Cl, and Sr increase exponentially in Zone-3 (Figure 7). In particular, three intervals from ~1,000 to 800 cal yr BP, ~600 to 300 cal yr BP, and ~150 cal yr BP to present exhibit very high hurricane activities. Coincidentally, the modern dense mangrove forest in southwestern Florida was established during the last millennia (Yao & Liu, 2017; Yao et al., 2015). Therefore, it is reasonable to believe that the increased mineral and sediment inputs due to elevated hurricane activities after 1,150 cal yr BP likely enhanced nutrient availabilities in the Shark River Estuary and played an important role in the development of the mangrove forests at our study area (Castañeda-Moya et al., 2020).

Overall, the geochemical data sets of core SRM identified 5 active periods of intense hurricane activities during the last 3,500 years at ~3,400–3,000, ~2,200–1,500, ~1,000–800, ~600–300, and ~150 cal yr BP to present (Figure 7). This is the longest paleohurricane record to date from South Florida. This study also demonstrates that geochemical signals, in particular, signals of saltwater intrusion can be preserved in the sediment profiles on millennial time-scale and measured by selected XRF variables, thereby enabling more storm records to be produced from otherwise suboptimal sand-limited coastal systems such as the Florida Everglades. This methodological advancement has the potential to connect the existing hurricane records in the regional context to examine the long-term hurricane dynamics at a regional scale.

For the isotopic results, previous studies have indicated that marine-originated organic materials, hence storm deposits, contain more positive $\delta^{13}C$ and lower C/N values (Figure 8) (Chmura & Aharon, 1995; Das et al., 2013; Lamb et al., 2006; Lambert et al., 2008). However, the inferred storm intervals show very inconsistent $\delta^{13}C$ and C/N values throughout Zone-2 and Zone-3 (Figure 7), and most intervals in core SRM-1 fall within the range of C3 terrestrial plants instead of marine originated sources (Figure 8). We think this discrepancy is caused by high contents of mangrove peat in the core. In our study area, the scarcity of clastic material (especially sand) and peat-dominated sediment profiles contributed to high content of TOC throughout core SRM-1 (Figure 5). More importantly, the peat deposition at the mouth of the Shark

River Slough was mainly contributed by autochthonous accumulation from the mangrove forests since ~3,500 cal yr BP (Lodge, 2016; Parkinson, 1989; Yao & Liu, 2017; Yao et al., 2015). In the Everglades, all three mangroves species that include *Laguncularia racemosa*, *Rhizophora mangle*, and *Avicennia germinans* are C3 plants. It is likely that strong $\delta^{13}C$ and C/N signals contributed by organic materials from mangrove peat overwhelm the occasional hurricane signals in the sediment profile.

4.3. Climatic Forcing and Late-Holocene Hurricane Activities in the Florida Everglades

Our paleohurricane record from the Everglades documented five active periods of intense hurricane activities at ~3,400–3,000, ~2,200–1,500, ~1,000–800, ~600–300, and ~150 cal yr BP to present. Many studies from across the GOM and Caribbean Basin have attributed the periodic changes in the regional climatic patterns (e.g., precipitation and hurricanes) during the Late-Holocene to variations of the Intertropical Convergence Zone (ITCZ) position, the position and strength of the Bermuda High or North Atlantic Oscillation (NAO), and/or intensification of the El Niño/Southern Oscillation (ENSO) (e.g., Aragón-Moreno et al., 2018; Baldini et al., 2016; Donnelly & Woodruff, 2007; Elsner et al., 2000; Hodell et al., 1991; Liu & Fearn, 2000; McCloskey & Liu, 2012a, 2012b). In addition to these large-scale climatic controls, it is important to point out that our study site, situated on the Gulf Coast of the Everglades, is affected by intense hurricanes coming from both the Atlantic Ocean to the east (i.e., the Cape Verde hurricanes) and the Gulf of Mexico to the west (i.e., the baroclinically enhanced hurricanes, such as Hurricane Wilma) (Elsner et al., 1996) (Figure 2). Therefore, the paleohurricane history of our study site may reflect the complex interactions among the different climatic mechanisms affecting the activity of the Cape Verde hurricanes versus the baroclinically-enhanced hurricanes either concurrently or asynchronously. Figure 9 shows our proxy-indicated activity periods plotted alongside some key paleoclimatic proxy records from the Caribbean and broader neotropical regions.

The first active period, ~3,400–3,000 cal yr BP, coincides with a distinct rise in $\delta^{18}O$ values at Lake Miragoane, Haiti (Figure 9c), interpreted to signal an abrupt shift toward a drier climate in the Caribbean (Hodell et al., 1991). This climatic change has been attributed to a southwestward shift of the Bermuda High, the subtropical anticyclone that steers many Cape Verde hurricanes from the tropical Atlantic Ocean toward North America (Liu & Fearn, 2000). Consequently, more hurricanes were steered toward the Gulf of Mexico and the Caribbean region after 3,800 cal yr BP, marking the onset of a hyperactive period in intense hurricane landfall detected in the paleotempestology records across the northern Gulf of Mexico coast (Liu, 2004). It is remarkable that the onset of heightened hurricane activity seemed to occur synchronously across the Gulf Coast, even down to the Everglades. It also coincided with a southward shift of the ITCZ around 3,500 cal yr BP (Haug et al., 2001). Thus, the paleoclimatic records seem to support that the 3,400–3,000 cal yr BP active period in the Everglades was part of a large-scale atmospheric circulation changes that involved a southward shift of the ITCZ and the Bermuda High around 3,500 years ago.

The second active period, ~2,200–1,500 cal yr BP, coincided with an abrupt increase in the Ca/Fe elemental ratio in the Rio Hondo record from the southeastern Yucatan Peninsula (Figure 9b), interpreted to reflect increased precipitation in the western Caribbean (Aragón-Moreno et al., 2018). Hurricane landfall along the northern Gulf of Mexico coast continued to be high (Bregy et al., 2018; Liu, 2004). At the same time, ENSO activity increased to the highest level during the late Holocene (Conroy et al., 2008), while the climate in Haiti remained dry (Hodell et al., 1991) (Figures 9c and 9d). One possible scenario is that the elevated activity recorded in the southwestern Everglades during this period was due to an increase in baroclinically enhanced hurricanes spawned from the Gulf of Mexico and the western Caribbean. The coupled effects of ITCZ movements and ENSO intensification on precipitation and hurricane activity in the Gulf of Mexico region are complex and not well known (Aragón-Moreno et al., 2018). More work is needed to evaluate this hypothesis.

All three of the youngest active periods occurred within the last millennium. Thus, the period 1,000–0 cal yr BP can be broadly regarded as a relatively active period. The interval of ~900–600 was also identified as a time of high hurricane activity in a proxy record near Naples, southwestern Florida, only 80 km north of our study site (Ercolani et al., 2015). By contrast, the last millennium was shown to be an inactive period marked by few intense hurricane landfalls on the northern Gulf Coast (Liu, 2004). A southward retreat of the ITCZ, as documented from the Cariaco Basin (Haug et al., 2001), would have caused a shift of the predominant storm tracks to the south, bringing fewer hurricanes to the northern Gulf Coast but more to the Everglades and to as far south as Nicaragua (McCloskey and Liu, 2012). On the other hand, the past

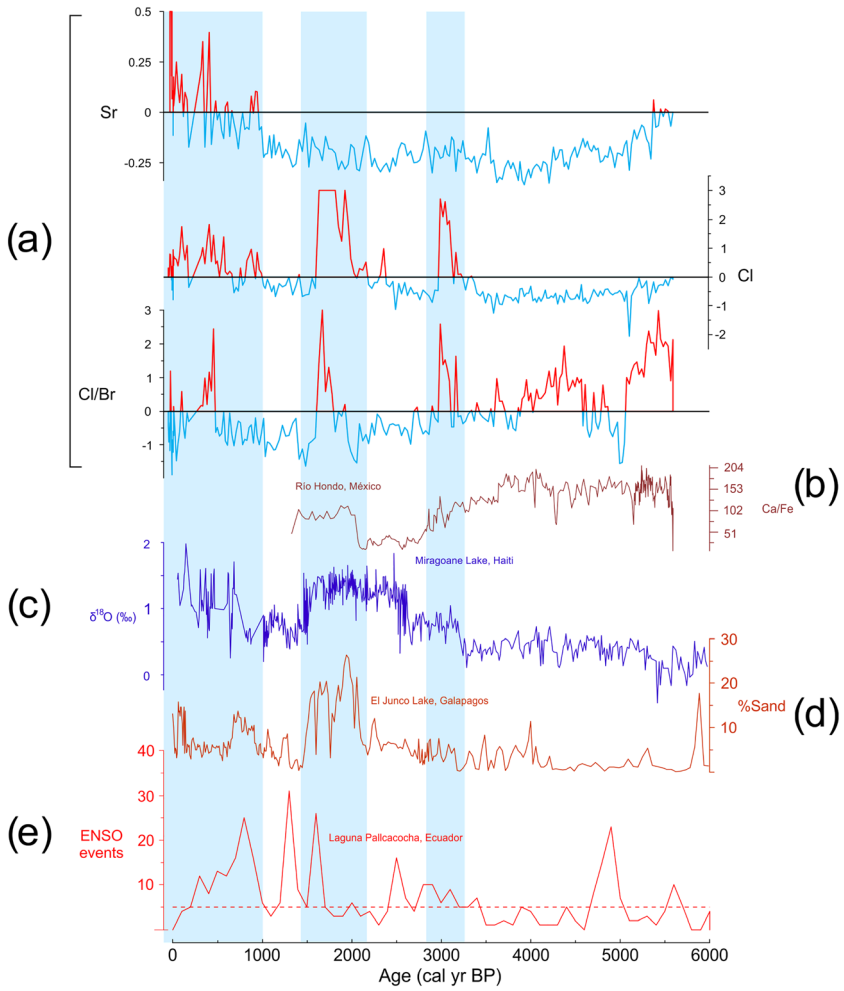

Figure 9. Paleohurricane record from (a) core SRM-1 comparing with other paleoenvironmental reconstructions from across the Caribbean and Eastern Pacific. (b) Precipitation record during the mid- to Late-Holocene from southeastern Yucatan Peninsula (Aragón-Moreno et al., 2018); (c) Holocene climate reconstructions of Lake Miragoane, Haiti based on $\delta^{18}O$ record (Hodell et al., 1991); (d) El Niño/Southern Oscillation (ENSO) intensifications during the Holocene interpreted by sand record from El Junco Lake, Galapagos (Conroy et al., 2008); (e) total ENSO events modeled by 100 years overlapping window from Laguna Pallcacocha, southern Ecuador (Moy et al., 2002). Intervals shaded in blue represent periods of elevated intense hurricane activities, ENSO intensifications, and increased precipitation in the Caribbean and Florida.

millennium seemed to be marked by moderately high ENSO activity in general, albeit with great variability (Conroy et al., 2008; Moy et al., 2002) (Figures 9d and 9e). On the submillennial level, the three active hurricane periods identified in our study site (~1,000–800, 600–300, and 150–0 cal yr BP) seem to correspond with intervals of relatively low ENSO activity (Figures 9d and 9e). Today, hurricane risks in South Florida are highest during years of positive Southern Oscillation Index (SOI) (or La Nina) and negative NAO (Elsner & Bossak, 2004). The apparent negative relationship between hurricane activity levels at our study site and the frequency of ENSO events suggests that hurricane activity regimes in South Florida have been modulated by the interplay among the ITCZ, ENSO, and NAO for at least the past millennium. It is likely that other regional climatic and oceanographic variables, such as the Loop Current and the Atlantic Multi-decadal Oscillation (AMO; which is largely a function of sea surface temperature in the tropical and subtropical Atlantic Ocean), may have played a significant role too (Bregy et al., 2018; Goldenberg et al., 2001).

In addition, the overall values of the marine indicators (Ca, Sr, and Zr) all increased after ~1,000 cal yr BP in core SRM-1 (Figure 5), approximately when the shoreline reached its modern position at the Shark River

Estuary (Yao et al., 2015). We believe that these marine sediments are likely carbonate materials contributed by small-scale events (e.g., winter storms and minor tropical cyclones) that produced an amalgamated deposit of material over time with the same chemical signals as deposits from intense hurricanes. As the approximate distance of site SRM-1 to the Gulf was relatively closer in the last millennia, our study area became more sensitive to receive and preserve deposits from these small-scale events in the sedimentary profile. However, the remarkable chemical imprints from the intense hurricanes such as Wilma is still clearly distinguishable as shown in the standardized data sets in Figure 7.

Many proxy-based paleohurricane records have been published from study sites along the Gulf Coast and the Caribbean in recent years (Baldini et al., 2016; Brandon et al., 2013; Bregy et al., 2018; Burn & Palmer, 2015; Das et al., 2013; Denommee et al., 2014; Donnelly & Woodruff, 2007; Ercolani et al., 2015; Frappier et al., 2007, 2014; Lane et al., 2011, 2017; LeBlanc et al., 2017; Liu et al., 2008; McCloskey & Liu, 2012a, 2012b, 2013; Park, 2012; van Hengstum et al., 2014; Wallace & Anderson, 2010; Wallace et al., 2014). These studies generally show multicentennial periods of significantly increased hurricane activity separated by quieter inactive periods during the Late-Holocene. Two hypotheses exist regarding the temporal correlations between the Late-Holocene active/inactive hurricane periods and the climatic forcing mechanisms. One group of views is that hurricane regimes are synchronous across the entire North Atlantic basin because hurricane activity levels are controlled by large-scale forcing mechanism such as ENSO, which affects the entire basin (Donnelly & Woodruff, 2007; Mann et al., 2009). Another group of views is that hurricane regimes are not synchronous across the North Atlantic. but instead, they show anti-phase or time-transgressive patterns across geographical regions as a result of latitudinal shifts in predominant storm tracks driven by changing positions or strengths of the ITCZ, Bermuda High, or NAO (Baldini et al., 2016; Elsner et al., 2000; Liu, 2004; Liu & Fearn, 2000; McCloskey & Liu, 2012a, 2012b; McCloskey et al., 2013). Our paleohurricane record is broadly in line with hurricane regimes inferred from records from Hancock County, Mississippi (Bregy et al., 2018); Apalachee Bay, North Florida (Lane et al., 2011); Southwest Florida (Ercolani et al., 2015); Belize (Denommee et al., 2014; McCloskey & Liu, 2012a); and Nicaragua (McCloskey & Liu, 2012b). Although the timing and length of the various active hurricane periods among the above records vary, the age gaps may be caused by various geomorphological and meteorological factors, dating control, and sensitivity of different study sites, rather than variations of the climatic forcing.

5. Conclusion

In this study, geochemical data sets from core SRM-1 and significance testing of 45 surface samples from the Shark River Estuary identified five active periods of intense hurricane activities during the last 3,500 years at ~3,400–3,000, ~2,200–1,500, ~1,000–800, ~600–300, and ~150–0 cal yr BP. Our results support the notion that intense hurricane activities in South Florida and the Gulf of Mexico/western Caribbean region were modulated by ITCZ movements, ENSO activities, and the NAO during the Late-Holocene. This study presents the longest hurricane record to date from South Florida. Hence, it fills an important data gap in the paleotempestology data network between the GOM and Atlantic Coasts of the United States and the Caribbean region. This study also contributes to the methodological advancement of paleotempestology by exploring the application of geochemical proxies in nonlimnic, sand-limited, and mangrove-dominated tropical coastal wetlands. Further paleoecological studies are needed to produce a high-resolution multiproxy record that integrates geochemical, sedimentological, and palynological data for a better understanding of the post-storm process of forest succession and ecosystem recovery in the Everglades during the Late-Holocene. More work also needs to be done to explore the use of geochemical and isotopic analyses in detecting storm signals from sand-limited coastal environments.

Acknowledgments

This research was supported by grants from the U.S. National Science Foundation (grants 1759715, 1212112, and NSF DDRI grant BCS-1303114) and the Inter-American Institute for Global Change Research (IAI SGP-CRA-2050). We thank T.A. McCloskey for his assistance in fieldwork. Special thanks go to the Florida Coastal Everglades LTER program, the Florida Bay Interagency Science Center-Everglades National Park (FBISC-ENP), and Florida International University for field and logistical support during this study. We also thank four anonymous reviewers who provided valuable comments to improve the manuscript. Data related to this article are open to the public and can be found at the Neotoma Paleoecology Database for free (https://www.neotomadb.org, Site ID: 10436).

References

Alcalá, F. J., & Custodio, E. (2008). Using the Cl/Br ratio as a tracer to identify the origin of salinity in aquifers in Spain and Portugal. *Journal of Hydrology*, *359*(1–2), 189–207.

Aragón-Moreno, A. A., Islebe, G. A., Roy, P. D., Torrescano-Valle, N., & Mueller, A. D. (2018). Climate forcings on vegetation of the southeastern Yucatán Peninsula (Mexico) during the middle to late Holocene. *Palaeogeography, Palaeoclimatology, Palaeoecology*, *495*, 214–226.

Baldini, L. M., Baldini, J. U. L., McElwaine, J. N., Frappier, A. B., Asmerom, Y., Liu, K.-B., et al. (2016). Persistent northward North Atlantic tropical cyclone track migration over the past five centuries. *Scientific Reports*, *6*(1), 37522. https://doi.org/10.1038/srep37522

Bianchette, T. A., McCloskey, T. A., & Liu, K.-B. (2016). Re-evaluating the geological evidence for Late Holocene marine incursion events along the Guerrero seismic gap on the Pacific Coast of Mexico. *PLoS ONE*, *11*(8), e0161568. https://doi.org/10.1371/journal.pone.0161568

Blaauw, M., & Christen, J. A. (2013). Bacon Manual e v2. 2. *Blaauw, M. , Wohlfarth, B. , Christen, JA, Ampel, L. , Veres, D. , Hughen, KA, Preusser, F. , et Al. (2010),—Were last glacial climate events simultaneous between Greenland and France*, 387–394.

Brandon, C. M., Woodruff, J. D., Lane, D. P., & Donnelly, J. P. (2013). Tropical cyclone wind speed constraints from resultant storm surge deposition: A 2500 year reconstruction of hurricane activity from St. Marks, FL. *Geochemistry, Geophysics, Geosystems*, *14*, 2993–3008. https://doi.org/10.1002/ggge.20217

Bregy, J. C., Wallace, D. J., Minzoni, R. T., & Cruz, V. J. (2018). 2500-year paleotempestological record of intense storms for the northern Gulf of Mexico, United States. *Marine Geology*, *396*, 26–42. https://doi.org/10.1016/j.margeo.2017.09.009

Burn, M. J., & Palmer, S. E. (2015). Atlantic hurricane activity during the last millennium. *Scientific Reports*, *5*(1), 12,838. https://doi.org/10.1038/srep12838

Castañeda-Moya, E., Rivera-Monroy, V. H., Chambers, R. M., Zhao, X., Lamb-Wotton, L., Gorsky, A., et al. (2020). Hurricanes fertilize mangrove forests in the Gulf of Mexico (Florida Everglades, USA). *Proceedings of the National Academy of Sciences*, *117*(9), 4831–4841. https://doi.org/10.1073/pnas.1908597117

Castañeda-Moya, E., Twilley, R. R., & Rivera-Monroy, V. H. (2013). Allocation of biomass and net primary productivity of mangrove forests along environmental gradients in the Florida Coastal Everglades, USA. *Forest Ecology and Management*, *307*, 226–241. https://doi.org/10.1016/j.foreco.2013.07.011

Castañeda-Moya, E., Twilley, R. R., Rivera-Monroy, V. H., Zhang, K., Davis, S. E., & Ross, M. (2010). Sediment and nutrient deposition associated with Hurricane Wilma in mangroves of the Florida Coastal Everglades. *Estuaries and Coasts*, *33*(1), 45–58. https://doi.org/10.1007/s12237-009-9242-0

Chen, R., & Twilley, R. R. (1999a). A simulation model of organic matter and nutrient accumulation in mangrove wetland soils. *Biogeochemistry*, *44*(1), 93–118. https://doi.org/10.1007/BF00993000

Chen, R., & Twilley, R. R. (1999b). Patterns of mangrove forest structure and soil nutrient dynamics along the Shark River estuary, Florida. *Estuaries*, *22*(4), 955–970. https://doi.org/10.2307/1353075

Chmura, G. L., & Aharon, P. (1995). Stable carbon isotope signatures of sedimentary carbon in coastal wetlands as indicators of salinity regime. *Journal of Coastal Research*, *11*(1), 124–135.

Conroy, J. L., Overpeck, J. T., Cole, J. E., Shanahan, T. M., & Steinitz-Kannan, M. (2008). Holocene changes in eastern tropical Pacific climate inferred from a Galápagos lake sediment record. *Quaternary Science Reviews*, *27*(11–12), 1166–1180. https://doi.org/10.1016/j.quascirev.2008.02.015

Craighead, F. C., & Gilbert, V. C. (1962). The effects of Hurricane Donna on the vegetation of southern Florida. *Quarterly Journal of the Florida Academy of Sciences*, *25*(1), 1–28.

Das, O., Wang, Y., Donoghue, J., Xu, X., Coor, J., Elsner, J., & Xu, Y. (2013). Reconstruction of paleostorms and paleoenvironment using geochemical proxies archived in the sediments of two coastal lakes in northwest Florida. *Quaternary Science Reviews*, *68*, 142–153. https://doi.org/10.1016/j.quascirev.2013.02.014

Davis, S. N., Whittemore, D. O., & Fabryka-Martin, J. (1998). Uses of chloride/bromide ratios in studies of potable water. *Ground Water*, *36*(2), 338–350. https://doi.org/10.1111/j.1745-6584.1998.tb01099.x

Denommee, K. C., Bentley, S. J., & Droxler, A. W. (2014). Climatic controls on hurricane patterns: A 1200-y near-annual record from Lighthouse Reef, Belize. *Scientific Reports*, *4*(1), 1–7.

Donahoe, R., Liu, C., Dobson, K., & Graham, E. (1994). Cycling of iron and manganese in a Riparian wetland. *Mineralogical Magazine*, *58*(1), 237–238.

Donnelly, J. P., Roll, S., Wengren, M., Butler, J., Lederer, R., & Webb, T. (2001). Sedimentary evidence of intense hurricane strikes from New Jersey. *Geology*, *29*(7), 615–618. https://doi.org/10.1130/0091-7613(2001)029<0615:SEOIHS>2.0.CO;2

Donnelly, J. P., & Woodruff, J. D. (2007). Intense hurricane activity over the past 5,000 years controlled by El Niño and the West African monsoon. *Nature*, *447*(7143), 465–468. https://doi.org/10.1038/nature05834

Dunn, G. E. (1965). The hurricane season of 1964. *Monthly Weather Review*, *93*(3), 175–187. https://doi.org/10.1175/1520-0493-93.3.175

Dunn, G. E., & Miller, B. I. (1961). The hurricane season of 1960. *Monthly Weather Review*, *89*(3), 99–108. https://doi.org/10.1175/1520-0493-89.3.99

Elsner, J. B., & Bossak, B. H. (2004). Hurricane landfall probability and climate. In R. J. Murnane, & K. B. Liu (Eds.), *Hurricanes and typhoons: Past, present and future* (333–353). New York, NY: Columbia University Press.

Elsner, J. B., & Kara, A. B. (1999). *Hurricanes of the North Atlantic: Climate and society*, Oxford, UK: Oxford University Press.

Elsner, J. B., Lehmiller, G. S., & Kimberlain, T. B. (1996). Objective classification of Atlantic hurricanes. *Journal of Climate*, *9*(11), 2880–2889. https://doi.org/10.1175/1520-0442(1996)009<2880:OCOAH>2.0.CO;2

Elsner, J. B., Liu, K. B., & Kocher, B. (2000). Spatial variations in major US hurricane activity: Statistics and a physical mechanism. *Journal of Climate*, *13*(13), 2293–2305. https://doi.org/10.1175/1520-0442(2000)013<2293:SVIMUS>2.0.CO;2

Ercolani, C., Muller, J., Collins, J., Savarese, M., & Squiccimara, L. (2015). Intense Southwest Florida hurricane landfalls over the past 1000 years. *Quaternary Science Reviews*, *126*, 17–25. https://doi.org/10.1016/j.quascirev.2015.08.008

Frappier, A. B., Pyburn, J., Pinkey-Drobnis, A. D., Wang, X., Corbett, D. R., & Dahlin, B. H. (2014). Two millennia of tropical cyclone-induced mud layers in a northern Yucatán stalagmite: Multiple overlapping climatic hazards during the Maya Terminal Classic "megadroughts". *Geophysical Research Letters*, *41*, 5148–5157. https://doi.org/10.1002/2014GL059882

Frappier, A. B., Sahagian, D., Carpenter, S. J., González, L. A., & Frappier, B. R. (2007). Stalagmite stable isotope record of recent tropical cyclone events. *Geology*, *35*(2), 111–114. https://doi.org/10.1130/G23145A.1

Gao, S., Jia, J. J., Yang, Y., Zhou, L., Wei, W., Mei, Y. (2019). Obtaining typhoon information from sedimentary records in coastal-shelf waters. *Haiyang Xuebao*, *41*(10), 141–160.

Glaser, P. H., Hansen, B. C. S., Donovan, J. J., Givnish, T. J., Stricker, C. A., & Volin, J. C. (2013). Holocene dynamics of the Florida Everglades with respect to climate, dustfall, and tropical storms. *Proceedings of the National Academy of Sciences of the United States of America*, *110*(43), 17,211–17,216. https://doi.org/10.1073/pnas.1222239110

Goldenberg, S. B., Landsea, C. W., Mestas-Nuñez, A. M., & Gray, W. M. (2001). The recent increase in Atlantic hurricane activity: Causes and implications. *Science*, *293*(5529), 474–479. https://doi.org/10.1126/science.1060040

Haug, G. H., Hughen, K. A., Sigman, D. M., Peterson, L. C., & Röhl, U. (2001). Southward migration of the intertropical convergence zone through the Holocene. *Science*, *293*(5533), 1304–1308. https://doi.org/10.1126/science.1059725

Hodell, D. A., Curtis, J. H., Jones, G. A., Higuera-Gundy, A., Brenner, M., Binford, M. W., & Dorsey, K. T. (1991). Reconstruction of Caribbean climate change over the past 10, 500 years. *Nature*, *352*(6338), 790–793. https://doi.org/10.1038/352790a0

Houston, S. H., & Powell, M. D. (2003). Surface wind fields for Florida Bay hurricanes. *Journal of Coastal Research*, *19*(3), 503–513.

Lamb, A. L., Wilson, G. P., & Leng, M. J. (2006). A review of coastal palaeoclimate and relative sea-level reconstructions using δ13C and C/N ratios in organic material. *Earth-Science Reviews*, *75*(1–4), 29–57. https://doi.org/10.1016/j.earscirev.2005.10.003

Lambert, J. W., Aharon, P., & Rodriguez, A. B. (2008). Catastrophic hurricane history revealed by organic geochemical proxies in coastal lake sediments: A case study of Lake Shelby, Alabama (USA). *Journal of Paleolimnology*, *39*(1), 117–131. https://doi.org/10.1007/s10933-007-9101-6

Landsea, C. W., Franklin, J. L., McAdie, C. J., Beven, J. L., Gross, J. M., Jarvinen, B. R., et al. (2004). A reanalysis of hurricane Andrew's intensity. *Bulletin of the American Meteorological Society*, *85*(11), 1699–1712. https://doi.org/10.1175/BAMS-85-11-1699

Lane, C. S., Hildebrandt, B., Kennedy, L. M., LeBlanc, A., Liu, K.-B., Wagner, A. J., & Hawkes, A. D. (2017). Verification of tropical cyclone deposits with oxygen isotope analyses of coeval ostracod valves. *Journal of Paleolimnology*, *57*(3), 245–255. https://doi.org/10.1007/s10933-017-9943-5

Lane, P., Donnelly, J. P., Woodruff, J. D., & Hawkes, A. D. (2011). A decadally-resolved paleohurricane record archived in the late Holocene sediments of a Florida sinkhole. *Marine Ecology*, *287*(1–4), 14–30. https://doi.org/10.1016/j.margeo.2011.07.001

LeBlanc, A. R., Kennedy, L. M., Liu, K. B., & Lane, C. S. (2017). Linking hurricane landfalls, precipitation variability, fires, and vegetation response over the past millennium from analysis of coastal lagoon sediments, southwestern Dominican Republic. *Journal of Paleolimnology*, *58*(2), 135–150. https://doi.org/10.1007/s10933-017-9965-z

Liu, K. B. (2007). *Paleotempestology, Encyclopedia of Quaternary Science* (1978–1986). Oxford: Elsevier.

Liu, K. B. (2004). Paleotempestology: Principles, methods and examples from Gulf coast lake sediments. In R. J. Murnane, & K. B. Liu (Eds.), *Hurricanes and typhoons: Past, present and future* (13–57). New York, NY: Columbia University Press.

Liu, K. B. (2013). Paleotempestology. In S. A. Elias (Ed.), *The encyclopedia of quaternary science* (Vol. 3, pp. 209–221). Oxford, UK: Elsevier.

Liu, K. B., & Fearn, M. L. (1993). Lake-sediment record of late Holocene hurricane activities from coastal Alabama. *Geology*, *21*(9), 793–796. https://doi.org/10.1130/0091-7613(1993)021<0793:LSROLH>2.3.CO;2

Liu, K. B., & Fearn, M. L. (2000). Reconstruction of prehistoric landfall frequencies of catastrophic hurricanes in northwestern Florida from lake sediment records. *Quaternary Research*, *54*(2), 238–245. https://doi.org/10.1006/qres.2000.2166

Liu, K. B., Lu, H., & Shen, C. (2008). A 1200-year proxy record of hurricanes and fires from the Gulf of Mexico coast: Testing the hypothesis of hurricane–fire interactions. *Quaternary Research*, *69*(1), 29–41. https://doi.org/10.1016/j.yqres.2007.10.011

Liu, K. B., McCloskey, T. A., Ortego, S., & Maiti, K. (2015). Sedimentary signature of Hurricane Isaac in a Taxodium swamp on the western margin of Lake Pontchartrain, Louisiana, USA. *Proceedings of the International Association of Hydrological Sciences*, *367*, 421–428.

Lodge, T. E. (2016). *The everglades handbook: Understanding the ecosystem*, Boca Raton, FL: CRC Press. https://doi.org/10.1201/9781315369037

Mann, M. E., Woodruff, J. D., Donnelly, J. P., & Zhang, Z. (2009). Atlantic hurricanes and climate over the past 1,500 years. *Nature*, *460*(7257), 880–883. https://doi.org/10.1038/nature08219

Mayfield, M., Avila, L., & Rappaport, E. N. (1994). Atlantic hurricane season of 1992. *Monthly Weather Review*, *122*(3), 517–538. https://doi.org/10.1175/1520-0493(1994)122<0517:AHSO>2.0.CO;2

McCloskey, T. A., Bianchette, T. A., & Liu, K. B. (2013). Track patterns of landfalling and coastal tropical cyclones in the Atlantic Basin, their relationship with the North Atlantic Oscillation (NAO), and the potential effect of global warming. *American Journal of Climate Change*, *02*(03), 12–222. https://doi.org/10.4236/ajcc.2013.23A002

McCloskey, T. A., Bianchette, T. A., & Liu, K. B. (2015). Geological and sedimentological evidence of a large tsunami occurring ~1100 year BP from a small coastal lake along the Bay of La Paz in Baja California Sur, Mexico. *Journal of Marine Science and Engineering*, *3*(4), 1544–1567, Retrieved from. http://www.mdpi.com/2077-1312/3/4/1544/htm

McCloskey, T. A., & Liu, K. B. (2012a). A 7000 year record of paleohurricane activity from a coastal wetland in Belize. *Holocene*, *23*(2), 278–291. https://doi.org/10.1177/0959683612460782

McCloskey, T. A., & Liu, K. B. (2012b). A sedimentary-based history of hurricane strikes on the southern Caribbean coast of Nicaragua. *Quaternary Research*, *78*(3), 454–464. https://doi.org/10.1016/j.yqres.2012.07.003

McCloskey, T. A., & Liu, K. B. (2013). Sedimentary history of mangrove cays in Turneffe Islands, Belize: Evidence for sudden environmental reversals. *Journal of Coastal Research*, *29*(4), 971–983.

McCloskey, T. A., Smith, C. G., Liu, K. B., Marot, M., & Haller, C. (2018). How could a freshwater swamp produce a chemical signature characteristic of a saltmarsh? *ACS Earth and Space Chemistry*, *2*(1), 9–20. https://doi.org/10.1021/acsearthspacechem.7b00098

Moy, C. M., Seltzer, G. O., Rodbell, D. T., & Anderson, D. M. (2002). Variability of El Niño/Southern Oscillation activity at millennial timescales during the Holocene epoch. *Nature*, *420*(6912), 162–165. https://doi.org/10.1038/nature01194

Naquin, J. D., Liu, K. B., McCloskey, T. A., & Bianchette, T. A. (2014). Storm deposition induced by hurricanes in a rapidly subsiding coastal zone. *Journal of Coastal Research*, *70*, 308–313. https://doi.org/10.2112/SI70-052.1

NOAA. (2019). NOAA Historical Hurricane Tracks. Retrieved November 26, 2019, from https://oceanservice.noaa.gov/news/historical-hurricanes/

Park, L. E. (2012). Comparing two long-term hurricane frequency and intensity records from San Salvador Island, Bahamas. *Journal of Coastal Research*, 891–902. https://doi.org/10.2112/jcoastres-d-11-00065.1

Parkinson, R. W. (1989). Decelerating Holocene sea-level rise and its influence on Southwest Florida coastal evolution; a transgressive/regressive stratigraphy. *Journal of Sedimentary Research*, *59*(6), 960–972. https://doi.org/10.1306/212f90c5-2b24-11d7-8648000102c1865d

Ramírez-Herrera, M.-T., Lagos, M., Hutchinson, I., Kostoglodov, V., Machain, M. L., Caballero, M., et al. (2012). Extreme wave deposits on the Pacific coast of Mexico: Tsunamis or storms?—A multi-proxy approach. *Geomorphology*, *139-140*, 360–371. https://doi.org/10.1016/j.geomorph.2011.11.002

Risi, J. A., Wanless, H. R., Tedesco, L. P., & Gelsanliter, S. (1995). Catastrophic sedimentation from Hurricane Andrew along the Southwest Florida Coast. *Journal of Coastal Research*, 83–102.

Ryu, J., Bianchette, T. A., Liu, K.-B., Yao, Q., & Maiti, K. D. (2018). Palynological and geochemical records of environmental changes in a Taxodium swamp near Lake Pontchartrain in southern Louisiana (USA) during the last 150 years. *Journal of Coastal Research*, *85*, 381–385.

Salkind, N. J. (2010). *Encyclopedia of research design* (Vol. 2, Thousand Oaks, CA: SAGE Publications, Inc.

Scholl, D. W., Craighead, F. C. Sr., & Stuiver, M. (1969). Florida submergence curve revised: Its relation to coastal sedimentation rates. *Science*, *163*(3867), 562–564. https://doi.org/10.1126/science.163.3867.562

Simard, M., Zhang, K., Rivera-Monroy, V. H., Ross, M. S., Ruiz, P. L., Castañeda-Moya, E., et al. (2006). Mapping height and biomass of mangrove forests in Everglades National Park with SRTM elevation data. *Photogrammetric Engineering & Remote Sensing*, *72*(3), 299–311. https://doi.org/10.14358/PERS.72.3.299

Simpson, R. H., & Riehl, H. (1981). *The hurricane and its impact*, Baton Rouge, LA: Louisiana State University Press.

Smith, T. J., Anderson, G. H., Balentine, K., Tiling, G., Ward, G. A., & Whelan, K. R. T. (2009). Cumulative impacts of hurricanes on Florida mangrove ecosystems: Sediment deposition, storm surges and vegetation. *Wetlands*, *29*(1), 24–34. https://doi.org/10.1672/08-40.1

Smoak, J. M., Breithaupt, J. L., Smith, T. J., & Sanders, C. J. (2013). Sediment accretion and organic carbon burial relative to sea-level rise and storm events in two mangrove forests in Everglades National Park. *Catena*, *104*, 58–66. https://doi.org/10.1016/j.catena.2012.10.009

Tuthill, A. H., Avery, R. E., Lamb, S., & Kobrin, G. (1998). *Effect of chlorine on common materials in fresh water (No. CONF-980316)*, 37, 11–52). NACE International.

van Hengstum, P. J., Donnelly, J. P., Toomey, M. R., Albury, N. A., Lane, P., & Kakuk, B. (2014). Heightened hurricane activity on the Little Bahama Bank from 1350 to 1650 AD. *Continental Shelf Research*, *86*, 103–115. https://doi.org/10.1016/j.csr.2013.04.032

Van Soelen, E. E., Brooks, G. R., Larson, R. A., Sinninghe Damsté, J. S., & Reichart, G. J. (2012). Mid-to late-Holocene coastal environmental changes in southwest Florida, USA. *Holocene*, *22*(8), 929–938. https://doi.org/10.1177/0959683611434226

Wallace, D. J., & Anderson, J. B. (2010). Evidence of similar probablility of intense hurricane strikes for the Gulf of Mexico over the late Holocene. *Geology*, *38*(6), 511–514. https://doi.org/10.1130/G30729.1

Wallace, D. J., Woodruff, J. D., Anderson, J. B., & Donnelly, J. P. (2014). Palaeohurricane reconstructions from sedimentary archives along the Gulf of Mexico, Caribbean Sea and western North Atlantic Ocean margins. *Geological Society, London, Special Publications*, *388*(1), 481–501. https://doi.org/10.1144/SP388.12

Wanless, H. R., Parkinson, R. W., & Tedesco, L. P. (1994). Sea level control on stability of Everglades wetlands. In *Everglades: The ecosystem and its restoration* (pp. 199–223). Delray Beach, FL, USA: St. Lucie Press.

Westerhoff, P., Chao, P., Mash, H. (2004). Reactivity of natural organic matter with aqueous chlorine and bromine. *Water Research*, *38*. (6), 1502–1513. https://doi.org/10.1016/j.watres.2003.12.014

Whelan, K. R. T., Smith, T. J., Anderson, G. H., & Ouellette, M. L. (2009). Hurricane Wilma's impact on overall soil elevation and zones within the soil profile in a mangrove forest. *Wetlands*, *29*(1), 16–23. https://doi.org/10.1672/08-125.1

World Health Organization (2020). World Health Organization, Tropical cyclones. Retrieved March 26, 2020, from https://www.who.int/health-topics/tropical-cyclones#tab=tab_1

Williams, H., & Liu, K.-B. (2019). Contrasting Hurricane Ike washover sedimentation and Hurricane Harvey flood sedimentation in a southeastern Texas coastal marsh. *Marine Geology*, *417*, 106011. https://doi.org/10.1016/j.margeo.2019.106011

Woodruff, J. D., Donnelly, J. P., Mohrig, D., & Geyer, W. R. (2008). Reconstructing relative flooding intensities responsible for hurricane-induced deposits from Laguna Playa Grande, Vieques, Puerto Rico. *Geology*, *36*(5), 391–394. https://doi.org/10.1130/G24731A.1

Woodruff, J. D., Donnelly, J. P., & Okusu, A. (2009). Exploring typhoon variability over the mid-to-late Holocene: Evidence of extreme coastal flooding from Kamikoshiki, Japan. *Quaternary Science Reviews*, *28*(17-18), 1774–1785. https://doi.org/10.1016/j.quascirev.2009.02.005

Yao, Q., & Liu, K. B. (2017). Dynamics of marsh-mangrove ecotone since the mid-Holocene: A palynological study of mangrove encroachment and sea level rise in the Shark River Estuary, Florida. *PLoS ONE*, *12*(3), e0173670. https://doi.org/10.1371/journal.pone.0173670

Yao, Q., & Liu, K. B. (2018). Changes in modern pollen assemblages and soil geochemistry along coastal environmental gradients in the Everglades of South Florida. *Frontiers in Ecology and Evolution*, *5*, 178. https://doi.org/10.3389/fevo.2017.00178

Yao, Q., Liu, K. B., Platt, W. J., & Rivera-Monroy, V. H. (2015). Palynological reconstruction of environmental changes in coastal wetlands of the Florida Everglades since the mid-Holocene. *Quaternary Research*, *83*(3), 449–458. https://doi.org/10.1016/j.yqres.2015.03.005

Yao, Q., Liu, K. B., & Ryu, J. (2018). Multi-proxy characterization of hurricanes Rita and Ike storm deposits in the Rockefeller wildlife refuge, southwestern Louisiana. *Journal of Coastal Research*, *85*(SI), 841–845. https://doi.org/10.2112/SI85-169.1

Yao, Q., Liu, K. B., Williams, H., Joshi, S., Bianchette, T. A., Ryu, J., & Dietz, M. (2019). Hurricane Harvey storm sedimentation in the San Bernard National Wildlife Refuge, Texas: Fluvial versus storm surge deposition. *Estuaries and Coasts*, *43*(5), 971–983. https://doi.org/10.1007/s12237-019-00639-6

Zhang, K., Simard, M., Ross, M., Rivera-Monroy, V. H., Houle, P., Ruiz, P., et al. (2008). Airborne laser scanning quantification of disturbances from hurricanes and lightning strikes to mangrove forests in Everglades National Park, USA. *Sensors*, *8*(4), 2262–2292. https://doi.org/10.3390/s8042262

Zhou, L., Gao, S., Yang, Y., Zhao, Y., Han, Z., Li, G., et al. (2017). Typhoon events recorded in coastal lagoon deposits, southeastern Hainan Island. *Acta Oceanologica Sinica*, *36*(4), 37–45. https://doi.org/10.1007/s13131-016-0918-6

Zhou, L., Yang, Y., Wang, Z., Jia, J., Mao, L., Li, Z., et al. (2019). Investigating ENSO and WPWP modulated typhoon variability in the South China Sea during the mid–late Holocene using sedimentological evidence from southeastern Hainan Island, China. *Marine Geology*, *416*, 105987. https://doi.org/10.1016/j.margeo.2019.105987